5-10-2013

Electron transport in quantum dot chains: Dimensionality effects and hopping conductance

V. P. Kunets

Mariama Rebello Sousa Dias
University of Richmond, mdias@richmond.edu

T. Rembert

M. E. Ware

Y. I. Mazur

See next page for additional authors

Recommended Citation

Kunets, V.P., M.Rebello Sousa Dias, T. Rembert, M.E. Ware, Y.I. Mazur, V. Lopez-Richard, H. A. Mantooth, G.E. Marques, G.J. Salamo. "Electron transport in quantum dot chains: Dimensionality effects and hopping conductance." *Journal of Applied Physics* 113, 183709 (2013), doi: 10.1063/1.4804324.

Electron transport in quantum dot chains: Dimensionality effects and hopping conductance

Vas. P. Kunets,[1,a)] M. Rebello Sousa Dias,[2] T. Rembert,[1,3] M. E. Ware,[1] Yu. I. Mazur,[1] V. Lopez-Richard,[2,a)] H. A. Mantooth,[3] G. E. Marques,[2] and G. J. Salamo[1]
[1]*Institute for Nanoscience and Engineering, University of Arkansas, Fayetteville, Arkansas 72701, USA*
[2]*Departamento de Física, Universidade Federal de São Carlos, 13565 905 São Carlos, SP, Brazil*
[3]*Department of Electrical Engineering, University of Arkansas, Fayetteville, Arkansas 72701, USA*

(Received 30 January 2013; accepted 24 April 2013; published online 10 May 2013)

Detailed experimental and theoretical studies of lateral electron transport in a system of quantum dot chains demonstrate the complicated character of the conductance within the chain structure due to the interaction of conduction channels with different dimensionalities. The one-dimensional character of states in the wetting layer results in an anisotropic mobility, while the presence of the zero-dimensional states of the quantum dots leads to enhanced hopping conductance, which affects the low-temperature mobility and demonstrates an anisotropy in the conductance. These phenomena were probed by considering a one-dimensional model of hopping along with band filling effects. Differences between the model and the experimental results indicate that this system does not obey the simple one-dimensional Mott's law of hopping and deserves further experimental and theoretical considerations.

I. INTRODUCTION

Progress in nano-scale electronics architectures and the continuous search for ultra-small circuit components have resulted in increased interest in the unique properties of low-dimensional systems such as quantum wires (QWRs) and coupled quantum dots (QDs). Recently, using molecular-beam epitaxy and strain engineering, a unique system of aligned quantum dots, i.e., quantum dot chains (QDCs), were successfully synthesized.[1,2] In previous reports, using structural and optical characterization techniques, it was shown that the QDC systems have a complex band structure caused by the combination of two-dimensional (2D), one-dimensional (1D), and zero-dimensional (0D) densities of states.[3,4] In this regard, systems of 1D coupled QDs have attracted much attention both in order to understand the underlying physics[5] and to develop novel devices. The co-existence of 2D and 1D states, that are important for enhanced electrical conductivity, as well as 1D and 0D states, that can play a role in the suppression of thermal conductivity, also makes this system a potential target for development of thermoelectric applications.[6]

In this work, we study electron transport in a system of QDCs and compare it to 1D hopping models. The presence of 0D states on top of a 1D wetting layer (WL) makes the electron transport in QDCs different from a system of continuous wires. This results in a different anisotropic response as well as enhanced hopping at low temperatures. The transport was probed with respect to band filling phenomena by supplying various concentrations of free carriers through remote doping in the GaAs barriers. Thus, the effect of changing the relative position of the Fermi level can be determined.

II. EXPERIMENTAL

All samples were grown in a solid source, Riber 32P MBE system. After deposition of a 300 nm GaAs buffer layer onto a (100) semi-insulating GaAs substrate at 580 °C, the growth temperature was reduced to 540 °C for the deposition of 9 ML of $In_{0.48}Ga_{0.52}As$ to form a layer of QDs (see Fig. 1). The QDs were buried by 17.5 nm GaAs (the first half of the spacer layer) at the same temperature. Following this, the temperature was rapidly increased to 580 °C and the second half of the 17.5 nm GaAs spacer layer was deposited. The cycle was repeated 10 times to form rows of dots, aligned along the [110] crystal direction. The next 5 periods of QDCs were grown similarly with the addition of a Si-δ-doping layer in the middle of each GaAs barrier at the QD growth temperature of 540°C. The δ-doping layers were followed by 5 ML of low temperature

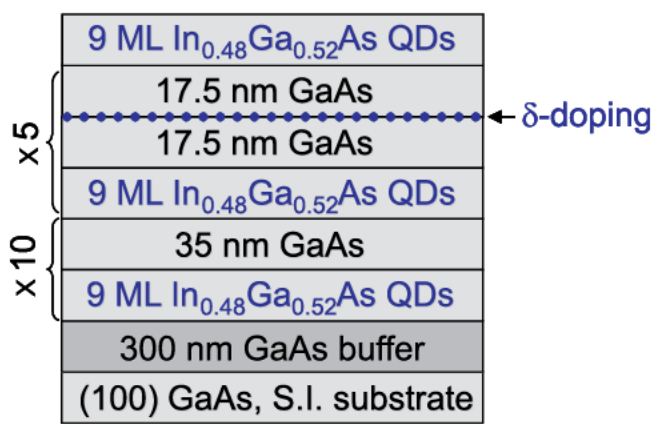

FIG. 1. Schematic of the layer structure of the QDC samples grown by MBE. The δ doping was located in the middle of each GaAs spacer layer only for the last 5 periods of growth. Three samples with different doping were prepared: sample A N_{2D} 1×10^{12} cm^{-2}, sample B N_{2D} 7.5×10^{11} cm^{-2}, and sample C N_{2D} 5×10^{11} cm^{-2}.

a)Authors to whom correspondence should be addressed. Electronic addresses: vkunets@uark.edu and vlopez@df.ufscar.br.

(540 °C) GaAs to ensure an abrupt doping profile. After which, the rest of the GaAs spacer was grown at 580 °C, again following a rapid temperature rise. Each sample was capped with an unburied layer of InGaAs QDs for AFM studies. Three samples were grown with varying doping concentration: sample A with $N_{2D} = 1 \times 10^{12}$ cm ^{2}, sample B with $N_{2D} = 7.5 \times 10^{11}$ cm ^{2}, and sample C with $N_{2D} = 5 \times 10^{11}$ cm ^{2}.

III. RESULTS AND DISCUSSION

Figure 2 presents representative atomic force microscope (AFM) images of the QDCs in our samples. The long chains of InGaAs QDs are well organized parallel ($\parallel$) to the [1 1 0] crystallographic direction over long distances and perpendicular ($\perp$) to the [1 1 0] direction which runs across the chains. AFM analysis of the surface QDCs, Figs. 2(c) 2(e), has

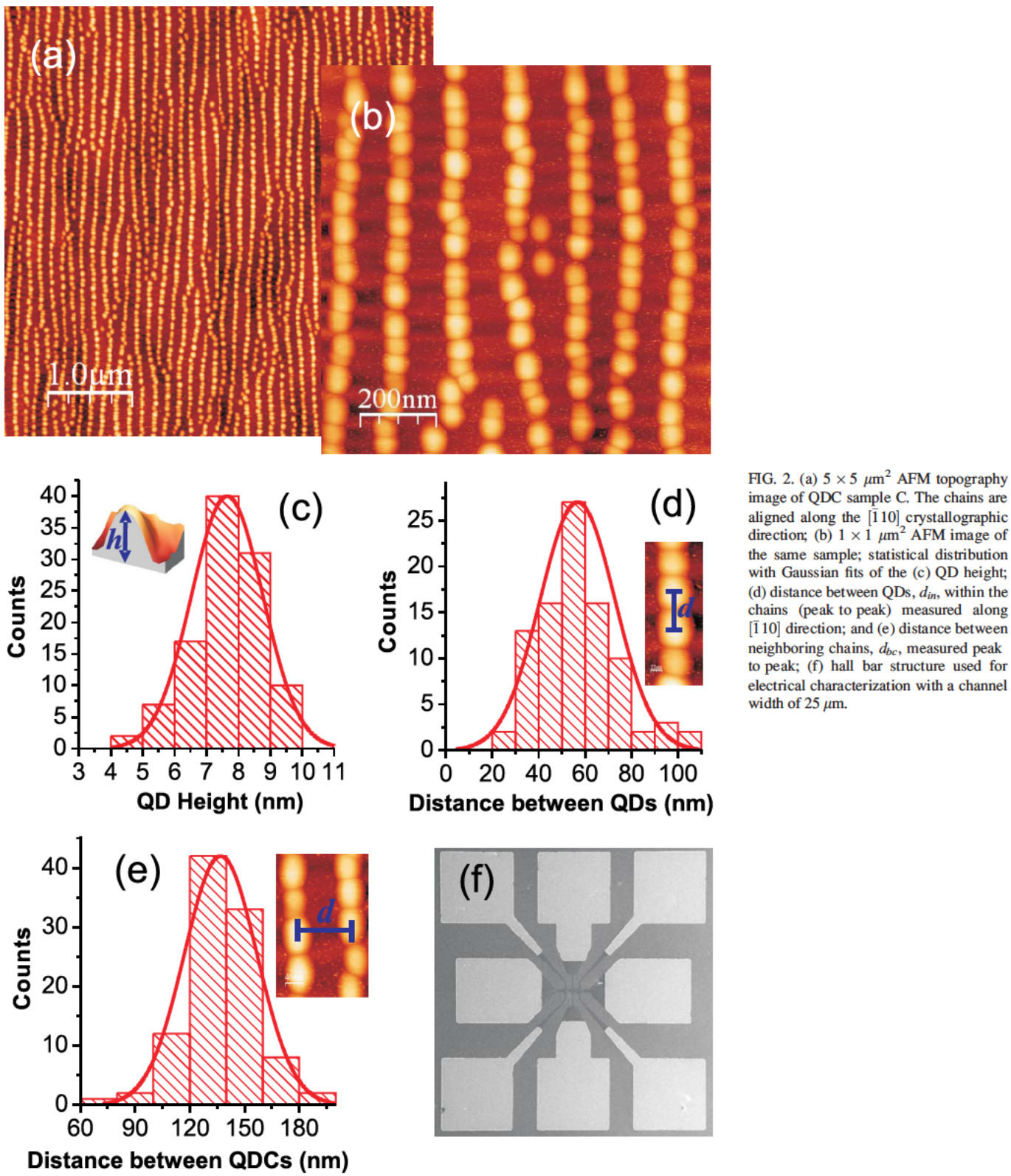

FIG. 2. (a) 5×5 μm^2 AFM topography image of QDC sample C. The chains are aligned along the $[\bar{1}10]$ crystallographic direction; (b) 1×1 μm^2 AFM image of the same sample; statistical distribution with Gaussian fits of the (c) QD height; (d) distance between QDs, d_{in}, within the chains (peak to peak) measured along $[\bar{1}10]$ direction; and (e) distance between neighboring chains, d_{bc}, measured peak to peak; (f) hall bar structure used for electrical characterization with a channel width of 25 μm.

revealed the average height of the QDs, the average radius of the QDs, the average spacing of the QDs within a chain, and the average chain to chain spacing to be: $h \sim 7.6$ nm, $r \sim 27$ nm, $d_{ic} \sim 57$ nm, and $d_{bc} \sim 137$ nm, respectively. These dimensions are important for understanding the electronic structure of the system and the underlying anisotropy. All of these structural parameters of the QDC systems have a normal distribution and are well fit by Gaussians.

The conductance in this system is governed by two main factors: (i) available states of different dimensionality and (ii) the position of the Fermi surface across the entire structure. In order to understand the role of these factors, let us first discuss possible conduction mechanisms through the states of different dimensionalities that lead to channels with different transmission probabilities. The total conductivity in the system of QDCs can be written as

$$\sigma_\xi = \sigma^{3DGaAs} + \sigma^{2DWL} + \sigma_\xi^{1DWL} + \sigma_\xi^{0D}, \tag{1}$$

where ξ denotes the [110] and [1$\bar{1}$0] directions. The conductivity in bulk GaAs, σ^{3DGaAs}, and in the 2D InGaAs wetting layer, σ^{2DWL}, are considered to be isotropic. The main source of anisotropy will be that due to the 1D wetting layer, $\sigma_{ij}^{1D,WL}$, formed due to the strain fields developed in-plane and along the growth direction.[3,4] The difference, $\Delta\sigma^{1DWL} = \sigma_{[110]}^{1DWL} - \sigma_{[1\bar{1}0]}^{1DWL} > 0$, is determined not only by the lateral confinement in the [110] direction but also by the lateral chain spacing in the [1$\bar{1}$0] direction, d_{bc}. Indeed, due to the high lateral spacing, $d_{bc} = 137$ nm, transport through 1D states in the [110] direction is only possible with the participation of the 2D states of the InGaAs WL and the 3D states of GaAs.[7]

In order to assess the anisotropy and the temperature dependence of the mobility of carriers through the QDs, we will consider a model based on hopping transport[8–12] that will take into account the structural parameters of our samples. Using the QDs as localization centers for charge carriers, the dot-to-dot transport along the chain or from chain-to-chain occur when an electron gains enough energy to escape into the barrier by absorbing phonons. Here, we consider a system of 10 chains with 1724 QDs each, in other words, we have calculated the mobility of a system of 10 by 1724 confining sites (QDs) by considering hopping between them. Labelling the QDs with an index, k, their occupation density is given by the Fermi-Dirac distribution

$$n_k = \frac{1}{1 + e^{\beta(\Delta + (k\ \ 1)V)}}, \tag{2}$$

where $\beta = (k_b T)^{\ 1}$, k_B is Boltzmann's constant, V is the drop in energy of each site due to an applied voltage, and $\Delta = \epsilon - \epsilon_f$ is the energy difference between the hopping energy state and the Fermi energy.

According to Miller and Abrahams,[8] the transition rate for hops from one site to another with relative position vector $\mathbf{r}_{kl}$ is given by

$$R_{kl} = \begin{cases} \nu_0 e^{\ a|\mathbf{r}_{kl}|\ \ \beta(\epsilon_l\ \ \epsilon_k)}, & \epsilon_l > \epsilon_k \\ \nu_0 e^{\ a|\mathbf{r}_{kl}|}, & \epsilon_l < \epsilon_k \end{cases}, \tag{3}$$

where ν_0 is an intrinsic transition rate, $a = 2/\alpha$ with α being the localization radius, and ϵ is the energy which includes the contribution of V. Therefore, the mobility can be calculated as

$$\mu_\xi = \frac{r_0}{\mathbf{E}\langle n_k^0 \rangle} \sum_k \sum_l [\mathbf{r}_{kl} R_{kl}^{(\xi)} n_k (1 - n_l) + \mathbf{r}_{kl} R_{kl}^{(\xi)} n_l (1 - n_k)], \tag{4}$$

where $\mathbf{E}$ is an applied electric field, r_0 is the lattice constant, and n_k^0 is the equilibrium Fermi-Dirac distribution (r_{kl} and α are given in units of r_0).

Within a strictly hopping formalism using a uniform 1D chain, there are only two mechanisms which can cause the transport properties to vary with direction resulting in anisotropy: the anisotropic effects of the electron-phonon interaction and the effective number of parallel sites contributing to the hopping mobility in each direction. The effect of increasing the number of distant hops is displayed in Figs. 3(a) and 3(b) using the sample parameters as measured in Fig. 2. We calculated the mobility for both directions, across and along the chains, Figs. 3(a) and 3(b), respectively, with different numbers of neighbors contributing to the hopping mechanism. The index l, in Eq. (4), runs through the values 1 to l_{max} as indicated along each curve in Fig. 3, and where l_{max} is the maximum number of neighbors considered in the calculations. As we can see, the mobility increases as we include more nearest neighbor hopping sites in the calculations. By fixing the number of neighbors involved in the hopping, the

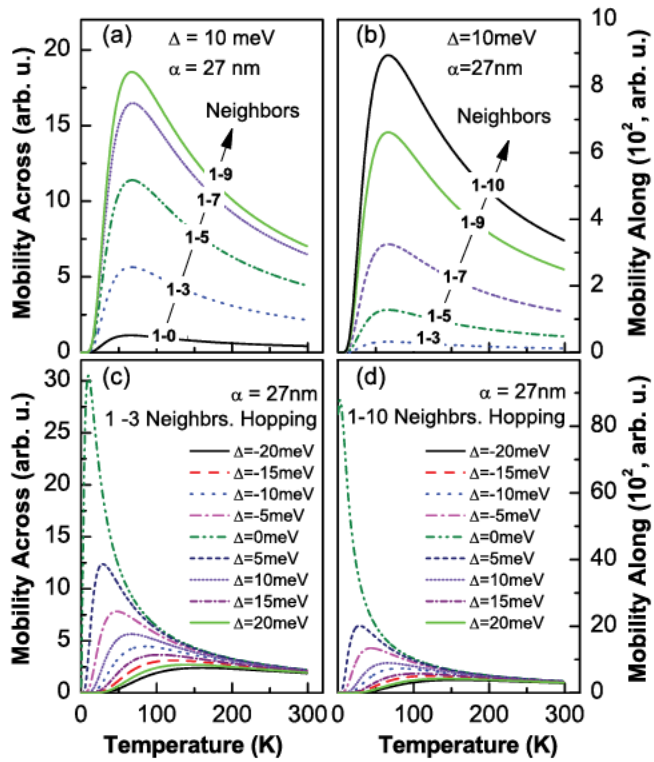

FIG. 3. Mobility versus temperature for α 27 nm. (a) Across the chains and (b) along the chains, both showing the effects of changing the number of neighbors involved in hopping. (c) Across the chain, for hops between the 3rd closest neighbors, varying Δ. (d) Along the chain, for hops between the 10th closest neighbors, varying Δ.

role of the parameter Δ, i.e., the Fermi level, in the mobility is assessed in Figures 3(c) and 3(d), across and along the chains, respectively. The farther the Fermi level is from the energy level of state which is being considered for hopping, the higher the temperature where the maximum mobility is attained. Such a behavior is attributed to the temperature dependence of the relative occupancy of the sites.

Now, we will demonstrate that this relative position of the Fermi energy impacts the anisotropic transport response of a system of 1D QDCs. We can calculate the conductance by considering just the first neighbor hopping.[9] The conductance in a 1D system of confining sites, the QDs, is equivalent to a model of conductors connected in series. The conductivity would then be

$$\sigma_\xi = N\alpha e^2 \beta \left[\sum_k \left(n_k (1 - n_k) R_{k,k+1}^{(\xi)} \right)^{1} \right]^{1}, \qquad (5)$$

where N is the number of sites. The anisotropic behavior will be assessed through the anisotropy ratio defined as $\eta = \sigma_{[1\bar{1}0]}/\sigma_{[110]}$, using Eq. (5) for the σ. Figure 4 shows the anisotropy ratio as a function of temperature and the relative position of the hopping state with respect to the Fermi energy, Δ. Note that this result is merely qualitative, since no attempt was made to include realistic values of the constants that enter Eqs. (3) and (5). A continuous increase of Δ produces qualitative changes on the anisotropy as a function of temperature. For lower values of Δ, the anisotropy ratio with temperature decreases monotonically while for higher values, the behavior becomes non-monotonic with a definite maximum. In the model, the Fermi energy and temperature appear combined within the Fermi-Dirac distribution. Thus, as expected for high temperatures, the carrier distribution is smeared and no essential differences can be observed in the occupation of neighboring sites and, thus, leading to a thermalized picture.

To study the conductance in our samples, we must force conduction through each of the systems of different dimensionality by moving the Fermi surface across each. We do this experimentally by using, temperature dependent Hall effect measurements. Figures 5(a) and 5(b) present the Hall mobility and electron sheet density, respectively, for our samples. These measurements were performed for each sample using Hall bars (see Fig. 2(f)) aligned along the [110] or [1$\bar{1}$0] crystallographic directions, i.e., across the QDCs or along them. Here, we find several distinct, noteworthy features: (i) the absolute value of the mobility is strongly dependent on remote doping concentration; (ii) the anisotropy is dependent on the temperature (Fig. 5(c)); and (iii) the low

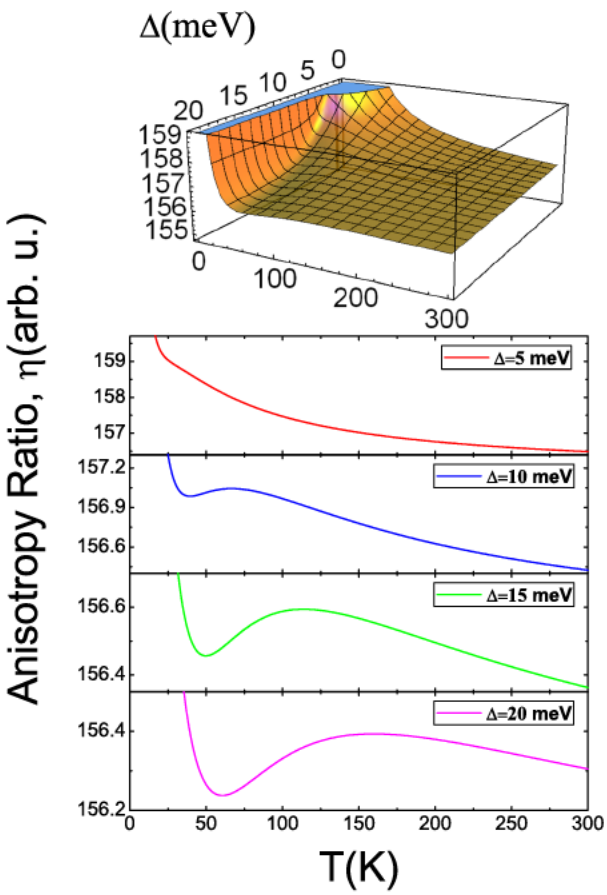

FIG. 4. Anisotropy ratio as a function of both temperature and Δ. The upper panel shows the complete 3D plot of this surface. The lower panel shows temperature profiles at different values of Δ. With the narrow vertical scale here, it is easy to see the evolution of the maxima of the anisotropy ratio as Δ increases.

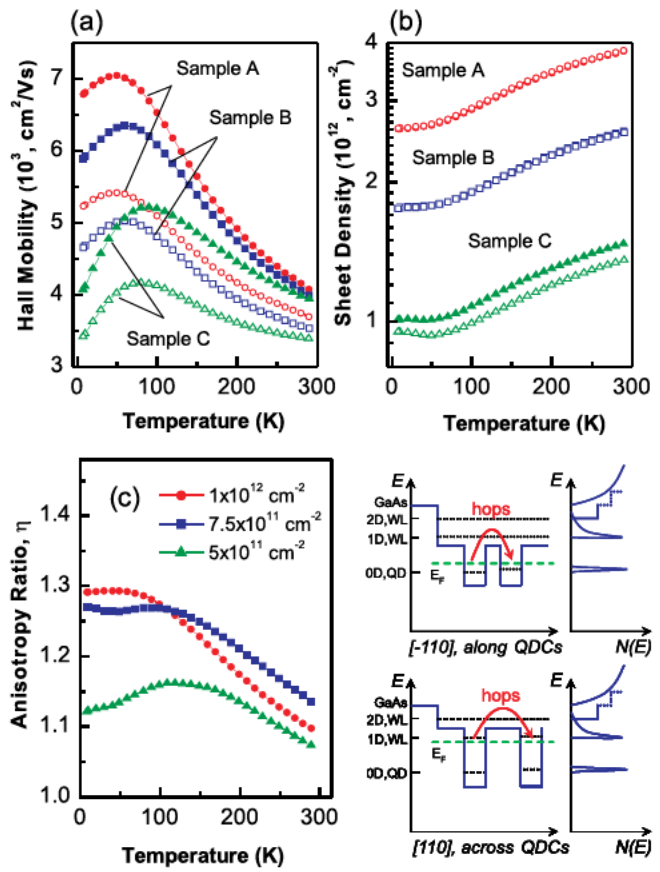

FIG. 5. (a) The Hall mobilities and (b) the electron sheet densities measured as a function of temperature for samples A, B, and C along the QDCs ([1$\bar{1}$0] direction, solid symbols) and across the QDCs ([110] direction, open symbols); (c) anisotropy as function of temperature and remote doping for samples A, B, and C. The inset shows a schematic band diagram in the (100) plane for [1$\bar{1}$0] (along QDCs) and [110] (across QDCs) crystallographic directions as well as the density of states diagrams.

temperature mobility ($T < 90$ K) progressively decreases with doping. At high temperatures, mobility along the chains shows only a slight variation with doping. At the same time, the high-temperature mobility across the QDC is obviously affected by the doping levels. This observed difference is small but is the result of the anisotropy in the conductivity of the 1D WL and of the QD chains. This is only observable due to the lowering of the Fermi energy with the decreasing doping level into the states of the lower dimensional systems. In other words, if the doping level was very high, into the GaAs conduction band, we expect to see no anisotropy in the conductivity.

At higher temperatures, we find as predicted from the 1D model in Fig. 3 that the mobilities decrease as the temperature rises. There are two effects which contribute to this decrease: the modulation of QD occupancy which inhibits hopping as described before and the increase in scattering rate by phonon interaction.[13] At temperatures below 100 K, the electron mobility reaches the maximum and starts to decrease again towards lower T. This decrease of mobility cannot be associated with enhanced scattering on ionized impurities at low temperatures because the thick spacer layers at 17.5 nm prevent this.[13] Instead, the mobility decrease here is due to the cross-over between 1D states in the InGaAs WL[7] and 0D states in the QDs. The decrease of doping and temperature makes these states dominant in charge transport. Hopping conduction becomes a dominant mechanism at lower temperatures which results in the observed drastic mobility decrease as T decreases. As predicted by the 1D model, the change in the Fermi level position by varying the doping density leads to the systematic shift of the mobility maximum.

Figure 5(c) presents the experimental results of the anisotropy, η, as functions of temperature and doping level. Notably, the QDCs behave differently with temperature and doping than a QWR system.[7] Our previous work on QWRs[7] showed that as the temperature decreases the anisotropy in the conductance increases and ultimately saturates. This was explained as the result of the dominating contribution of the 1D states as the Fermi level lowers in the low temperature regime.[7]

For QDCs, an interference of channels of a different nature may occur. The presence of QDs with 0D states effectively localizes carriers, reduces the charge transport in both [1 10] and [110] directions, and leads to the peculiar behavior displayed in Figure 5(c). At room temperature, for the highest remote doping of 1×10^{12} cm ^{2}, Sample A, the anisotropy is less than for the moderately doped Sample B, $N_{2D} = 7.5 \times 10^{11}$ cm ^{2}. This is an indication that the isotropic 2D states of the InGaAs WL and even the GaAs contribute to the conductance in Sample A, while for sample B the lower Fermi energy enhances conduction in the anisotropic 1D states. However, for Sample C, the Fermi level is lowered further into the 0D states of the QDs where hopping conduction dominates. This leads to lower anisotropy.

For all samples, decreasing the temperature leads to an increase in anisotropy as expected due to pinning of the Fermi energy in the 1D states. However, for samples B and C at ~110 K, the anisotropy reaches its maximum and decreases slightly. This non-monotonic behavior is a signature which is expected for hopping (see Fig. 4). This behavior is enhanced in the lightly doped sample C, $N_{2D} = 5 \times 10^{11}$ cm ^{2}. This sample shows the smallest conductance anisotropy between the three samples; however, its temperature dependence is completely different than the one obtained for QWRs,[7] where the highest η was measured for the sample with the lowest doping level. This suggests that for conduction in the QDC system the 0D states dominate over the 1D and 2D states. In sample C, at $T \sim 110$ K, the anisotropy rapidly starts to decrease with temperature, similar to sample B. This decrease of anisotropy with temperature as well as the sharp drop in mobility at low temperatures indicates that QDs dominate the transport. As shown by the schematic diagram in the inset of Fig. 5, when the Fermi energy is low enough and is in the 0D states of QDs, the transport will be governed by electron hopping in both the [110] and [1 10] directions.

Plotting the sheet resistance vs. the inverse temperature, Fig. 6, demonstrates dramatic differences between our samples. In both samples A and B, we see the normal increase in resistance at high temperatures due to increasing electron-phonon scattering. However, this is strongly suppressed for sample C where we find a continuous drop in resistance with increasing temperature.

Even though, the response of our samples matches qualitatively with the model of electron hopping, we would like to investigate the possibility of finding evidence of variable-range hopping[14] in our conductivity data. Ideally, this would obey Mott's law, which is given by

$$\sigma_{\xi}^{0D}(T) = \sigma_0^{(\xi)} \exp(-(T_0^{(\xi)}/T)^{x}). \tag{6}$$

Here, $T_0^{(\xi)} = 13.8/k_B N(\epsilon_f)\alpha^2$ which is determined by material properties, $N(\epsilon_f)$ is the density of states at the Fermi level, and $x = 1/3$ for phonon assisted hopping conductivity. The parameter $\sigma_0^{(\xi)} = \gamma^{(\xi)} T^m$, with $\gamma^{(\xi)}$ the temperature independent parameter reflecting the characteristic frequency of hopping "attempts" and $m =$ 1.[14–16] To characterize the

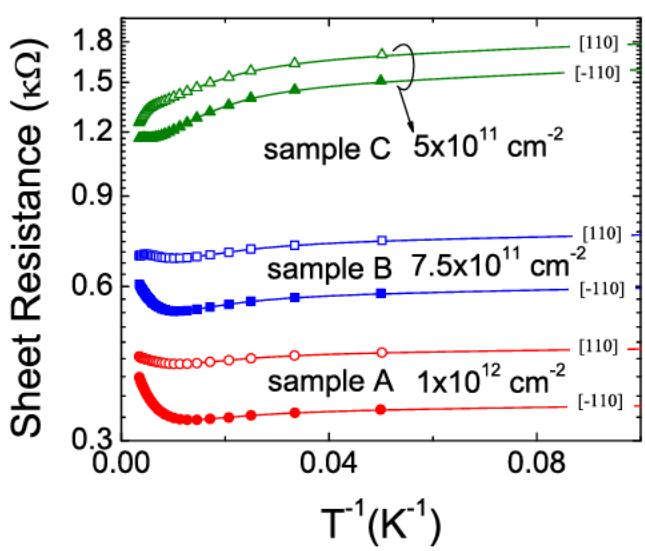

FIG. 6. (a) Sheet resistance as a function of inverse temperature.

temperature dependence of this variable-range hopping component of the conductivity $\sigma_{\xi}^{0D}(T)$, we followed the differential method proposed in Refs. 17 and 18, in which $\sigma_0^{(\xi)}$ is allowed to vary. In order to analyze the data, we consider the function[17]

$$W_{\xi}(T) = \partial \log \sigma_{\xi}(T)/\partial \log T = m + (T_0^{(\xi)}/T)^x. \quad (7)$$

For $m \ll x(T_0^{(\xi)}/T)^x$, we can write $\log W_{\xi}(T) = A_{\xi} - x \log T$, where $A_{\xi} = x \log T_0^{(\xi)}$. The plots of $\log W_{\xi}(T)$ vs. $\log T$ are shown in Fig. 7, for conduction both along and across the QDCs.

Certainly, a uniform 1D chain, as modelled before, cannot be fitted into the random picture of a disordered system where the variable-range hopping takes place. Thus, it is not surprising that the calculated values of $\log W_{\xi}(T)$ vs. $\log T$ differ from the Mott law already at low temperatures, as depicted in Figs. 7(a) 7(d). The behavior does not depend on the number of distant hops involved in the calculations, Figs. 7(a) and 7(b). Also, by varying Δ, the uniform chain response still deviates from the Mott law, Figs. 7(c) and 7(d), although the curves shift for each value of the relative hopping state position with respect to the Fermi energy.

Figures 7(e) and 7(f) show the experimental values of the mobility analyzed using Eq. (7). Deviations from the Mott behavior are predicted for variable-range hopping at low temperatures and obtained where a 1D ordering of sites in the chain creates a system size that is comparable to the typical length of a hop.[19–22] However, in our case, the divergence at lower temperatures does not fit into these predictions. Although, the curves in Figs. 7(e) and 7(f), are shifted analogously, in respect to the carrier concentration, as predicted by the theoretical calculations in Figs. 7(c) and 7(d). One may conclude that the qualitative discrepancy between experiments at low temperature with the Mott law and the 1D hopping model does not depend on the position of the Fermi energy. We were not able to determine the reason for such a behavior and this has opened an intensive search for a more systematic study of the conductivity in these QDCs. Certainly, the combination of various channels mask each other and assessing the nature of the main transport mechanisms within the whole temperature range is a task that requires further work.

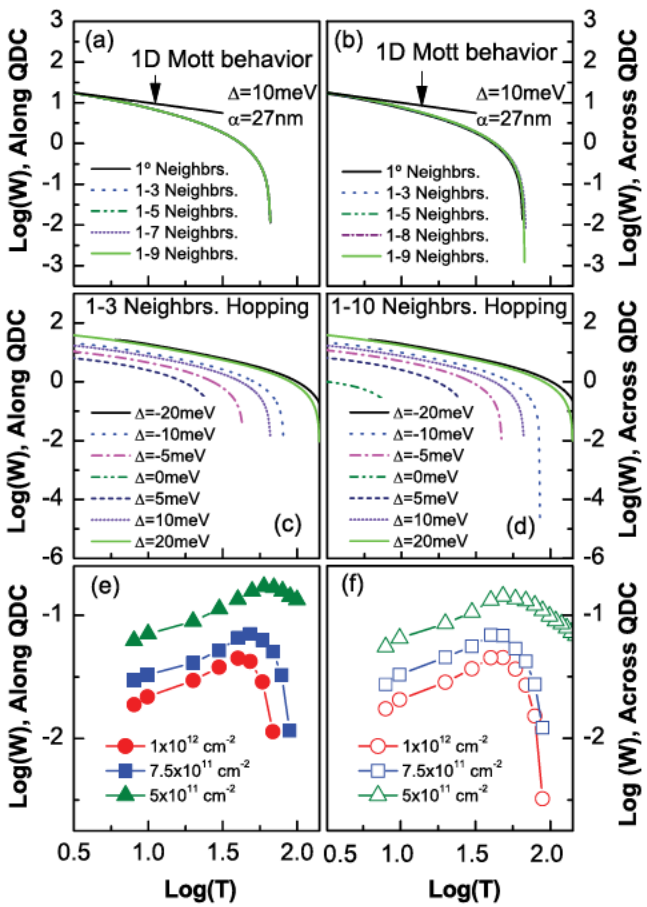

FIG. 7. $\log(W_{\xi})$ versus $\log(T)$. (a) and (b) along and across QD chain, respectively, with different number of hopping neighbors. The 1D Mott behavior (x 1/2) is shown by solid line. (c) and (d) along and across QD chain, respectively, where Δ is varying. (e) and (f) are experimental data.

For high doping levels, the conduction through energy levels of 1D and 2D systems may interfere. However, even for this case, conductivity, σ_{ξ}, is modulated by a hopping component of σ_{ξ}^{0D} through localized states in the QDs. For low doping levels, when the Fermi surface is mainly located in these 0D states, the hopping conductance is dominant and conduction through the 1D and 2D states is only possible through electrons scattered into higher energy states. Further decrease of sample temperature could bring our system into the regime of long-range Coulomb interaction, where hopping conduction is possible without phonon assistance. This will be a subject of our further studies.

IV. CONCLUSIONS

In summary, detailed studies of the mechanisms of conductance in a system of quantum dot chains as a function of temperature and remote doping level have been performed. We demonstrated that the behavior of the conductance is complicated due to the availability of states of different dimensionalities. We found that the presence of 0D states plays a key role in the anisotropic behavior of the conductance in this system and compared the experimental response to a 1D hopping model. At low temperatures, the experimental response of all samples deviates from Mott's law of conduction.

ACKNOWLEDGMENTS

This work was supported by the National Science Foundation through EPSCoR Grant No. EPS1003970. We acknowledge the support of the Brazilian agencies: FAPESP, CAPES, and CNPq.

[1]Zh. M. Wang, K. Holmes, Yu. I. Mazur, and G. J. Salamo, Appl. Phys. Lett. **84**, 1931 (2004).
[2]J. H. Lee, Zh. M. Wang, B. L. Liang, W. Black, Vas. P. Kunets, Yu. I. Mazur, and G. J. Salamo, Nanotechnology **17**, 2275 (2006).
[3]Yu. I. Mazur, W. Q. Ma, X. Wang, Zh. M. Wang, G. J. Salamo, M. Xiao, T. D. Mishima, and M. B. Johnson, Appl. Phys. Lett. **83**, 987 (2003).
[4]Zh. M. Wang, Yu. I. Mazur, J. L. Shultz, G. J. Salamo, T. D. Mishima, and M. B. Johnson, J. Appl. Phys. **99**, 033705 (2006).

[5]D. F. Cesar, M. D. Teodoro, V. Lopez Richard, G. E. Marques, E. Marega, Jr., V. G. Dorogan, Yu. I. Mazur, and G. J. Salamo, Phys. Rev. B **83**, 195307 (2011).
[6]L. D. Hicks and M. S. Dresselhaus, Phys. Rev. B **47**, 16631 (1993).
[7]Vas. P. Kunets, S. Prosandeev, Yu. I. Mazur, M. E. Ware, M. D. Teodoro, V. G. Dorogan, P. M. Lytvyn, and G. J. Salamo, J. Appl. Phys. **110**, 083714 (2011).
[8]A. Miller and E. Abrahams, Phys. Rev. **120**, 745 (1960).
[9]P. N. Bucher, *Linear and Nonlinear Electronic Transport in Solids*, edited by J. T. Devreese and V. E. Van Doren (Plenum, New York, 1976), pp. 341 381.
[10]B. I. Shklovskii and A. L. Efros, *Electronic Properties of Doped Semiconductors*, Springer Series in Solid State Science (Springer Verlag, 1984), Vol. 45.
[11]W. F. Pasveer, P. A. Bobbert, and M. A. J. Michels, Phys. Status Solidi C **1**, 164 (2004).
[12]W. Paschoal, Jr., S. Kumar, C. Borschel, P. Wu, C. M. Canali, C. Ronning, L. Samuelson, and H. Pettersson, Nano Lett. **12**, 4838 (2012).
[13]D. C. Look, *Electrical characterization of GaAs Materials and Devices* (John Wiley and Sons, New York, 1989).
[14]N. Mott, J. Non Cryst. Solids **1**, 1 (1968).
[15]D. N. Tsigankov and A. L. Efros, Phys. Rev. Lett. **88**, 176602 (2002).
[16]F. W. Van Keuls, X. L. Hu, H. W. Jiang, and A. J. Damm, Phys. Rev. B **56**, 1161 (1997).
[17]A. I. Yakimov, A. V. Dvurechenskii, A. I. Nikiforov, and A. A. Bloshkin, JETP Lett. **77**, 376 (2003).
[18]A. G. Zabrodskii and K. N. Zinov'eva, Sov. Phys. JETP **59**, 425 (1984).
[19]S. V. Zaitsev Zotov, Y. A. Kumzerov, Y. A. Firsov, and P. Monceau, J. Phys.: Condens. Matter **12**, L303 (2000).
[20]E. Slot, M. A. Holst, H. S. J. van der Zant, and S. V. Zaitsev Zotov, Phys. Rev. Lett. **93**, 176602 (2004).
[21]L. Venkataraman, Y. S. Hong, and P. Kim, Phys. Rev. Lett. **96**, 076601 (2006).
[22]Z. Zhou, K. Xiao, R. Jin, D. Mandrus, J. Tao, D. Geohegan, and S. Pennycook, Appl. Phys. Lett. **90**, 193115 (2007).